

Supporting Information

A. Modelling the basal plane and the prism planes of the Te nanorod

To model the prism and basal planes of the Te nanorods, we used symmetric periodic supercell slab models consisting of 3,6,9 and 12 atomic layers to find a representative model for the clean surface without Se adsorption. Finally we chose 9 atomic layers model with its five inner layers fixed. We calculated the optimized total energies of the Se/Te surface systems for various surface coverage of Se, using $p(2 \times 2)$ surface supercells, where the coverage of Se ranges from 0.25 to 1.00 monolayers (ML). In particular, the basal plane is represented by the (0001) surface of Te, while the prism plane is modeled using the (10 $\bar{1}$ 0) surface. These simplification is based on the crystal symmetry of Te nanorod, which has P 31 2 1 trigonal symmetry with hexagonal lattice. Covalently bonded tellurium atoms comprise a strand, and each strand forms van der Waals bonding with other strands. Its prism planes can be divided into two degenerate configurations due to its trigonal symmetry, and the two group share the same relative configuration due to the two fold symmetry. Therefore (10 $\bar{1}$ 0) facet alone can represent other five prism planes altogether. We also tested surface energy of (12 $\bar{1}$ 0) plane groups as well, and found that (10 $\bar{1}$ 0) gives lower surface free energy which means the better stability. This can be explained by the fact that the number of cut-off covalent bond is minimized for the planes belong to {10 $\bar{1}$ 0} family.

In order to estimate the effect of the surfactant and solvent environment, we used an *implicit* solvation model to calculate the solvation free energy due to the dielectric interaction between the surface and the surfactant, as implemented in VASPSol program.[S01] We approximated the relative dielectric constant of 4.0 to represent PVP, and 80.0 to represent deionized water in direct contact with the different facets. From the calculations, it is found that the solvation effect due to dielectric interaction is nominal in the Gibbs surface free energy results used in the main text. (see Figure S0 below) Still, it should be noted that the *explicit* role of PVP upon modifying the morphology of nanocrystal is not fully addressed in this *implicit* solvent model, such as selective binding effect.[S02]

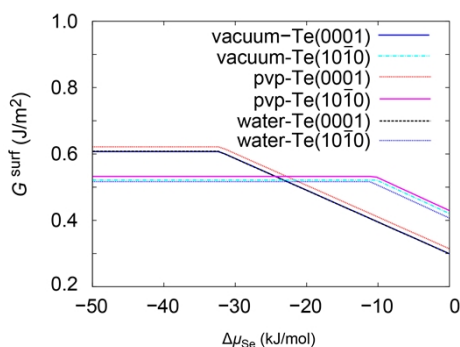


Figure S0. Solvation effect-induced Gibbs surface free energy diagram, due to chemical species in the reaction environment (PVP and DI-water), as described by the implicit solvation model. The relative dielectric constant of 4.0 is used for PVP, and 80.0 for DI-water.

B. Derivation to the calculation of the Gibbs surface free energy, Wulff shape, and the corresponding mole fraction of Selenium.

Adsorption energy per selenium atom:

$$E^{ad}(hktl, \theta, n^{Se}) = \frac{1}{n^{Se}} (E^{Se|Te}(hktl, \theta) - E^{Te}(hktl) - n^{Se} E_{bulk}^{Se})$$

Where $hktl$ denotes the Miller-Bravais 4-axis notation, and $t = -(h+k)$.

The surface of a tellurium facet can be calculated from the slab model as,

$$\sigma(hktl, \theta, s, n^{Se}) = \frac{1}{2A} (E^{Se|Te}(hktl, \theta, s) - E^{Te}(hktl) - n^{Se} E_{bulk}^{Se})$$

where $\sigma(hktl)$ is the surface energy, $E^{Se|Te}(hktl, \theta)$ is the calculated total energy from DFT calculation for the Te($hktl$) slab models with selenium atoms on the adsorption sites, θ is coverage in a unit of monolayer (ML), s is the variable for the adsorption site, $E^{Te}(hktl)$ is the total energy of the clean Te($hktl$) slab, n^{Se} is the number of selenium atoms, E_{bulk}^{Se} is the reference energy for the adsorbed selenium atom, which is taken to be the bulk phase of Se in this study.

Change in the Gibbs surface free energy with respect to varying chemical potential of the components can be expressed as following,

$$\Delta G^{surf}(hktl, \theta, s, n^{Se}, \Delta\mu^{Se}) = \frac{1}{2A} (E^{Se|Te}(hktl, \theta, s) - E^{Te}(hktl) - n^{Se} \Delta\mu^{Se} - n^{Te} \Delta\mu^{Te})$$

Note that ‘‘Change’’ refers to the change in Gibbs surface free energy due to adsorption of Selenium on the clean surface.

Therefore the full expression for the total Gibbs surface free is,

$$G^{surf} = \sigma + \Delta G^{surf}$$

Here we consider the change of chemical potential only for the adsorbate. Thus we approximated $\Delta\mu^{Te} \approx 0$.

Define the change in chemical potential of the Selenium with respect to its reference, (in this case, bulk Selenium) then it can be expressed as:

$$\Delta\mu^{Se} = \mu^{Se} - E_{ref}^{Se} = \mu^{Se} - E_{bulk}^{Se}$$

Reference values can be varied depending on the chemical conditions, and therefore one should not misinterpret the meaning of the zero value in the axis of chemical potential (x-axis). Since we set an approximation of invariable chemical potential of Te, therefore extremely high level of chemical potential of selenium will not represent the pure selenium state.

Now the change in Gibbs surface free energy can be expressed as:

$$\Delta G^{surf}(hktl, \theta, s, n^{Se}, \Delta\mu^{Se}) = \frac{1}{2A} (E^{Se|Te}(hktl, \theta, s) - E^{Te}(hktl) - n^{Se}(\Delta\mu^{Se} + E_{bulk}^{Se}))$$

Mind that,

$$E^{ad}(hktl, \theta, s, n^{Se}) = \frac{1}{n^{Se}} (E^{Se|Te}(hktl, \theta, s) - E^{Te}(hktl) - n^{Se} E_{bulk}^{Se})$$

We take the same reference of Selenium chemical potential reservoir in this study (i.e. bulk Selenium), Therefore,

$$\Delta G^{surf}(hktl, \theta, s, n^{Se}, \Delta\mu^{Se}) = \frac{n^{Se}}{2A} (E^{ad}(hktl, \theta, s, n^{Se}) - \Delta\mu^{Se})$$

and,

$$\begin{aligned} G^{surf}(hktl, \theta, s, n^{Se}, \Delta\mu^{Se}) &= \sigma(hktl) + \Delta G^{surf}(hktl, \theta, s, n^{Se}, \Delta\mu^{Se}) \\ &= \sigma(hktl) + \frac{n^{Se}}{2A} (E^{ad}(hktl, \theta, s, n^{Se}) - \Delta\mu^{Se}) \end{aligned}$$

By this, the Gibbs surface free energy has been derived as a linear function with respect to change in the chemical potential of selenium, $\Delta\mu^{Se}$.

From the equation, we can define multiple number of linearly decreasing G^{surf} functions, but we are only interested in the one with the lowest possible energy values. Therefore the observed Gibbs surface free energy can be derived as,

$$G^{surf}(hktl, \theta, s, n^{Se}, \Delta\mu^{Se}) = \sigma(hktl) + M(\Delta\mu^{Se})$$

where,

$$M(\Delta\mu^{Se}) = \min_{\Delta\mu^{Se} < 0} \left\{ \frac{n^{Se}}{2A} (E^{ad}(hktl, \theta, s, n^{Se}) - \Delta\mu^{Se}) \right\}$$

From these results, we can define the relationship between the thermodynamic descriptions of the surface energy of individual tellurium facet with respect to varying chemical potential of selenium in the chemical environment.

From the former discussion, we discuss two important calculation results, which correspond well with our experimental observations.

Firstly, the equilibrium crystalline shape (ECS) can be estimated by the Wulff construction. [S03]

$$\Delta G_i = \sum_j \sigma_j A_j$$

Where σ_j is the surface energy of j^{th} facet, and A_j is the area of the facet. From this definition, one can define a hypothetical construction in which exterior facets having normal vectors pointing to an origin, with the length of the j^{th} normal vector h_j as,

$$h_j = \lambda \sigma_j$$

And then the shape represents an equilibrium crystalline shape to which thermodynamic driving force exist.

Secondly, we provide a useful interpretation of the chemical potential change in terms of the mole fraction of the selenium used in the experiment.

We describe the chemical potential of i^{th} element in terms of chemical activity,

$$\mu^i = \mu_o^i + RT \ln a^i$$

where we used the ideal gas constant $R = 8.3144621 \text{ J} \cdot \text{K}^{-1} \cdot \text{mol}^{-1}$, T is the temperature, and the a^i is the chemical activity. The change in the chemical potential of selenium is,

$$\Delta \mu^{Se} = \mu^{Se} - \mu_{ref}^{Se}$$

Here, $\Delta \mu^{Se}$ is zero when the chemical potential of selenium reaches that of its reference state, which is, bulk state in this result. Then that can be expressed as,

$$\Delta \mu^{Se} = RT \ln X^{Se}$$

where it reaches zero when X^{Se} reaches one. Here we used the ideal gas constant for simplicity.

Finally, the mole fraction of X^{Se} can be calculated by,

$$X^{Se} = \exp\left(\frac{\Delta \mu^{Se}}{RT}\right)$$

[S01] K. Mathew, R. Sundararaman, K. Letchworth-Weaver, T. A. Arias, and R. G. Hennig, J. Chem. Phys. **140**, 084106 (2014).

[S02] P. S. Mdluli, N. M. Sosibo, P. N. Mashazi, T. Nyokong, R. T. Tshikhudo, A. Skepu, and E. Van Der Lingen, *J. Mol. Struct.* **1004**, 131 (2011).

[S03] G. Wulff, *Zeitschrift für Kristallographie-Crystalline Materials* **34**, 449 (1901).

C. Experimental Section

Materials. The chemicals used in this study were telluric acid ($\text{Te}(\text{OH})_6$, 99 %, Aldrich), selenous acid (H_2SeO_3 , 99 %, Aldrich), bismuth nitrate pentahydrate ($\text{Bi}(\text{NO}_3)_3 \cdot 5\text{H}_2\text{O}$, Aldrich), sodium hydroxide (NaOH , 93~99 %, Duksan), polyvinylpyrrolidone (PVP, $M_w \cong 55,000$, 99 %, Aldrich), hydroxylamine solution (w.t. 50 % in D. I. water, Aldrich), acetone (≥ 99.8 %, Aldrich), ethylene glycol (EG ≥ 99 %, J. T. Baker). D. I. water was obtained by an 18-M Ω (SHRO-plus DI) system.

Synthesis of Se_xTe_y alloys. To synthesize Se_xTe_y alloys, solvothermal method was used. Telluric acid and selenous acid (1.5 mmol in total with molar ratio $\text{Te}(\text{OH})_6/\text{H}_2\text{SeO}_3 = 100: 0, 99.7: 0.3, 99.3: 0.7, 99: 1$ and $98: 2$) were used as metal precursors. Sodium hydroxide (0.2 g (4 mmol)) and PVP (0.3 g (2.7 mmol)) were used. Above reagents were dissolved into 100ml of EG and poured into 250 ml round-bottom flask and stirred for 5 min for perfect mixture formation. Then 2.4 ml of hydroxyl amine solution were added at room temperature and flask was sealed with septa. Temperature was raised to 160 °C under nitrogen purging atmosphere and kept for 2 hours. After reaction, the solution was cooled down to room temperature and centrifuged (11,000 rpm, 10 min) 3 times using acetone (500 ml) and D. I. water (100 ml).

Kinetic observations. For observe kinetics of tellurium nanowire growth, telluric acid (0.345 g (1.5 mmol)), sodium hydroxide (0.2 g (4 mmol)) and PVP (0.3 g (2.7 mmol)) in 75 ml of EG were used for initial stage reaction. Hydroxylamine solution (2.4 ml) was mixed at room temperature and temperature was raised to 100 °C under nitrogen environment. Starting point of the reaction was set as the point of the solution temperature of 80 °C. Additional selenous acid (3.87 mg (30 μmol) in 5 ml of EG) was injected at 10/20/40 min after reaction starting point. Then, telluric acid (0.345 g (1.5 mmol) in 20 ml of EG) was injected into reaction mixture 160 min after reaction starting point. 0.5~1 ml of solution was taken out from reacting flask at 10/20/40/80/120/160/170/180/200/240/280/320 min and quenched down to R.T. and centrifuged 3 times for obtaining length profile through SEM observation. After reaction, the solution was cooled down to room temperature and centrifuged 3 times.

Formation of $\text{Bi}_2\text{Se}_x\text{Te}_y$ structures. For chemically transformed bismuth telluride structures, two-step procedure was used. First, Se_xTe_y alloys with various lengths and thicknesses were synthesized using morphology-controlling method introduced through this paper. After then bismuth precursor with stoichiometric ratio was injected for chemical transformation. In every case in **Figure 4**, basic experiment condition was identical to the kinetic observations part except reaction temperature of

100°C. To obtain thin and short case, selenous acid (9.675 mg (75 μmol) in 5 ml of EG) was injected at 5 min after reaction starting point. For thin and long case, tellurium nanorods are grown without any selenium injection. Thick and short case was obtained by using selenous acid (3.87 mg (30 μmol) and telluric acid (0.338 g (1.47 mmol)). Thick and long case was obtained by doing same procedure as thick and short case and after 120 min of reaction, telluric acid (0.345 g (1.5 mmol) in 20 ml of EG) was injected. All of the reactions were kept for 4 hours after final precursor injection of selenous acid or telluric acid. After then, bismuth nitrate pentahydrate (0.485 g (1 mmol) in 20 ml of EG, 0.970 g (2 mmol) for thick and long case) was injected into reacting flask and temperature was raised to 160 °C for perfect chemical transformation and kept for over 12 hours. After reaction, the solution was cooled down to room temperature and centrifuged 3 times.

Formation of PbSe_xTe_y structures. For chemically transformed lead telluride structures, two-step procedure was used. First, Se_xTe_y alloys with various lengths and thicknesses were synthesized using morphology-controlling method introduced through this paper. After then lead precursor with stoichiometric ratio was injected for chemical transformation. In every case in **Figure 5**, basic experiment condition was identical to the kinetic observations part except reaction temperature of 100°C. For thin and long case, tellurium nanorods are grown without any selenium injection. Thick and short case was obtained by using selenous acid (3.87 mg (30 μmol) and telluric acid (0.338 g (1.47 mmol)). After then, lead acetate trihydrate (0.569 g (1.5 mmol) in 20 ml of EG) was injected into reacting flask and temperature was set to 100 °C (160 °C for thick and short case) for perfect chemical transformation and kept for over 12 hours. After reaction, the solution was cooled down to room temperature and centrifuged 3 times.

D. Characterizations

Scanning electron microscopy (SEM) was run on a JEOL JSM-7001F field-emission scanning electron microscope operated at 15 kV. Transmission electron microscope (TEM) analysis was conducted with JEOL models (JEM-2010 and JEM-2100F) that were operated at 200 kV. X-ray diffraction was run on a RIGAKU Ultima IV.

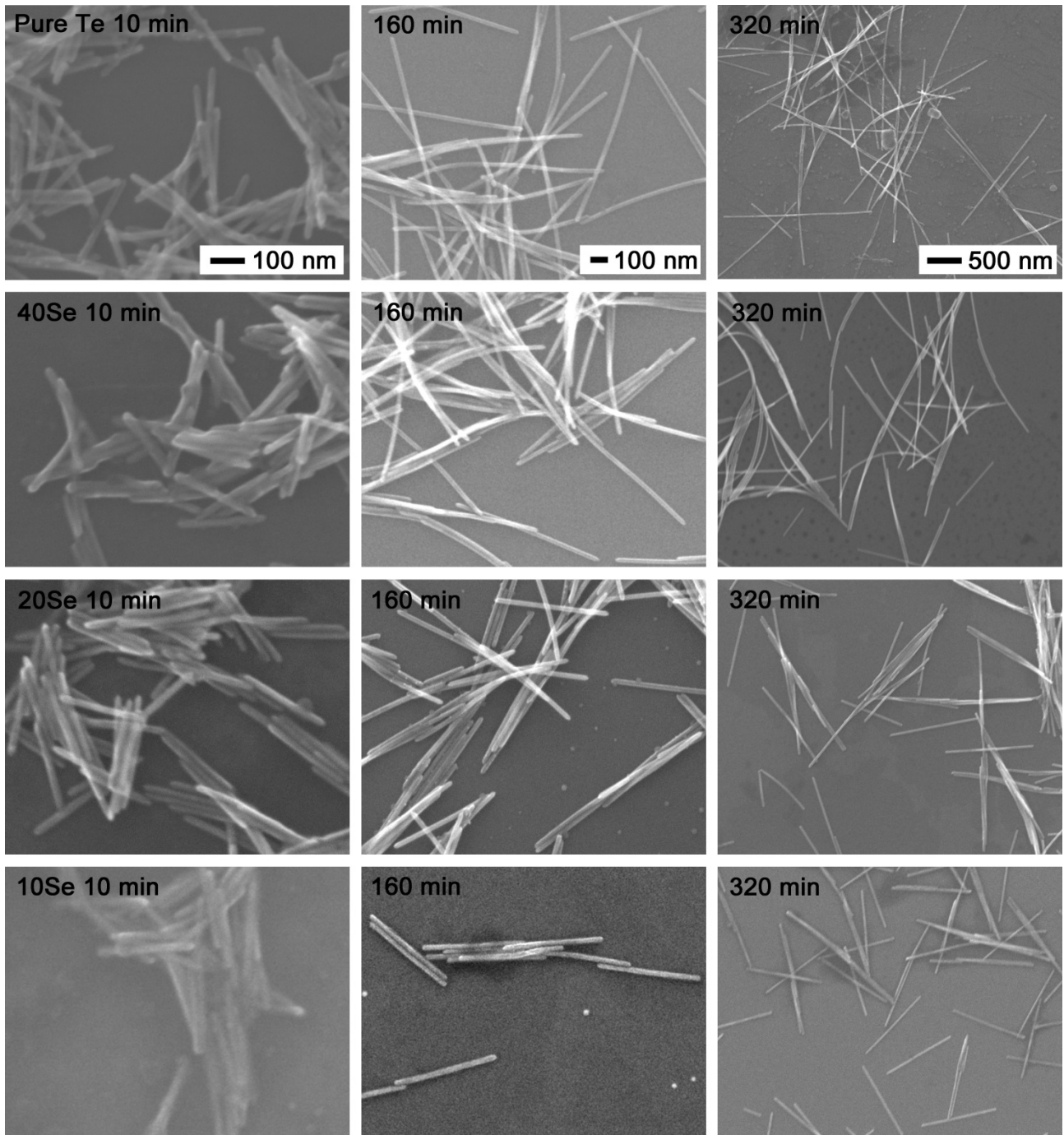


Figure S1. Length profile of nanowires in Figure 2 with respect to different selenium injection point and growth time.

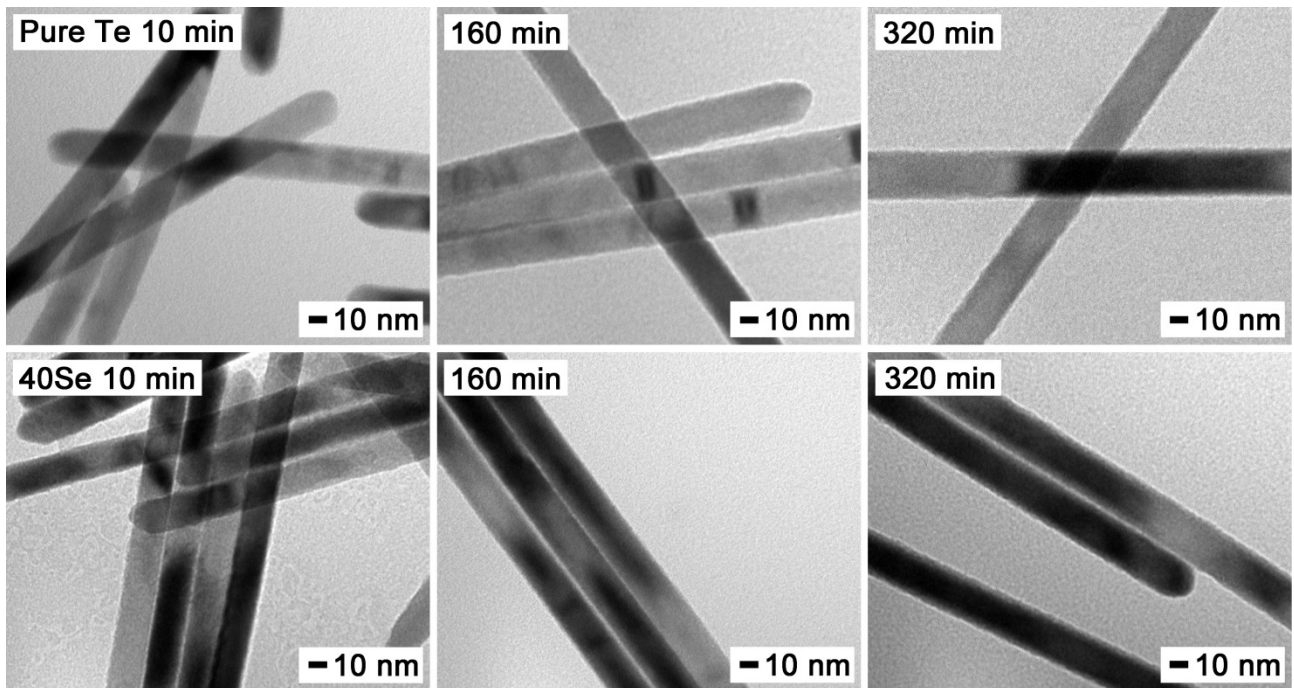


Figure S2. Diameter profile of nanowires in Figure 3 with respect to different selenium injection point and growth time.

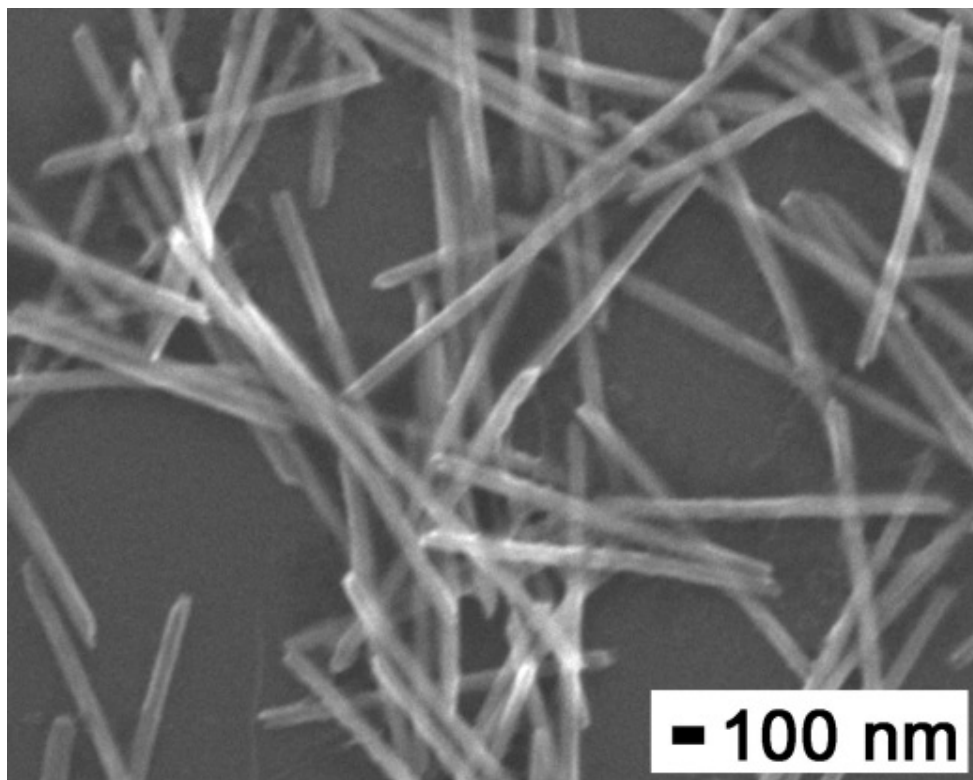


Figure S3. Te nanorods obtained from a supernatant solution of Se-doped Te nanorods. with supernatant of ‘Se injection (10 min)’ sample. Se was doped after 10 min reaction of the Te nanorods, and the reaction was allowed to proceed for 150 min. The solution was centrifuged and the supernatant solution were transferred into another reaction batch. An excess amount of reductant (5 ml of hydroxyl amine solution, 50 v/v%) was added to the new reaction batch. Temperature was raised to 120 °C and the reaction was kept for 60 min.

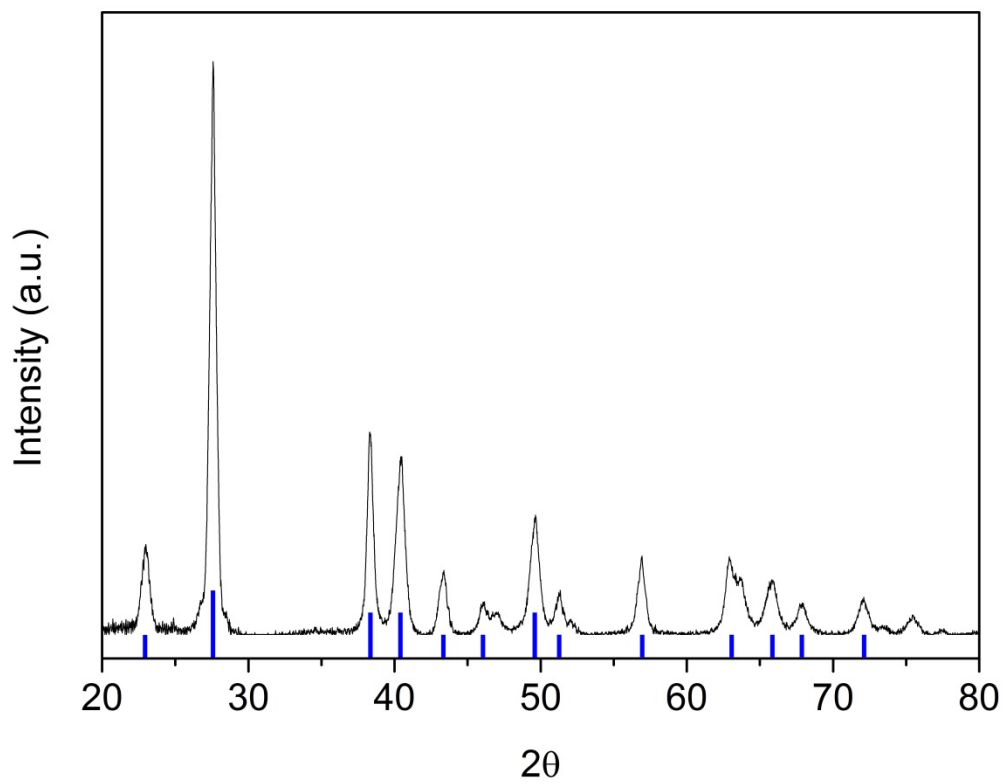


Figure S4. X-ray diffraction result of Te nanorods in Figure 4.

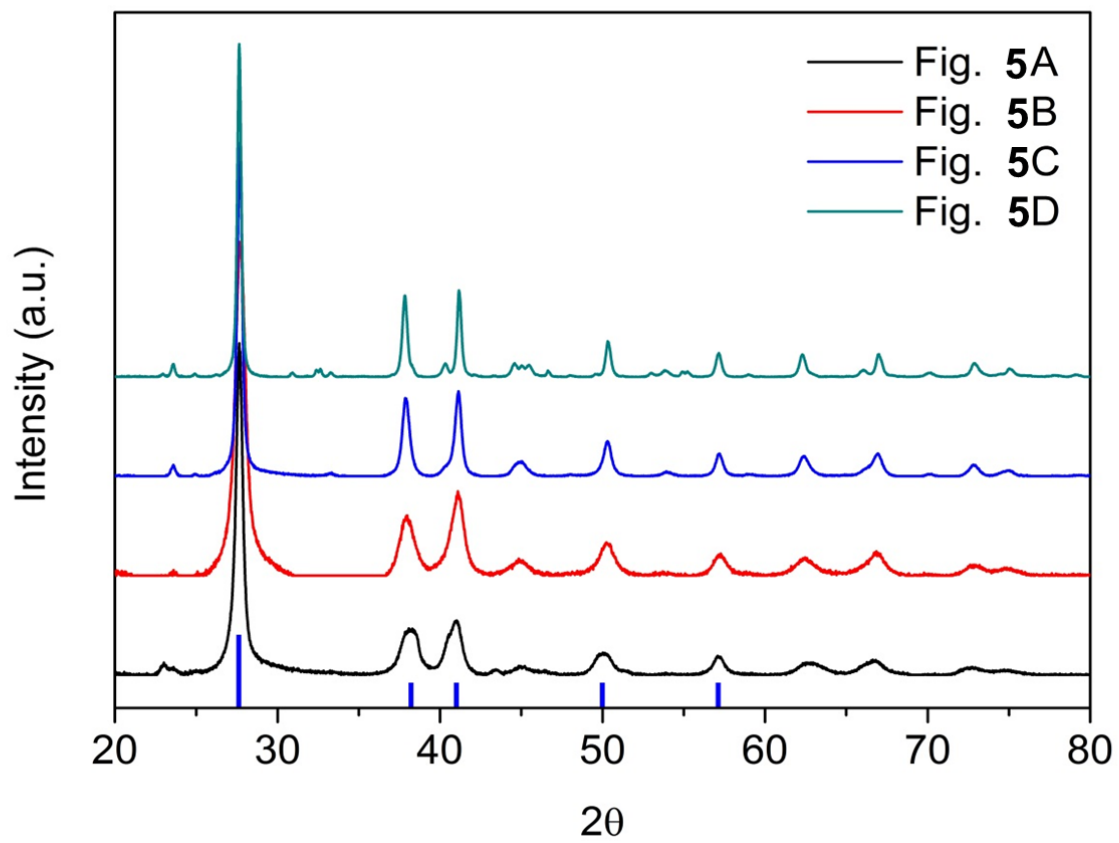


Figure S5. X-ray diffraction result of Bi_2Te_3 nanostructures in Figure 5.

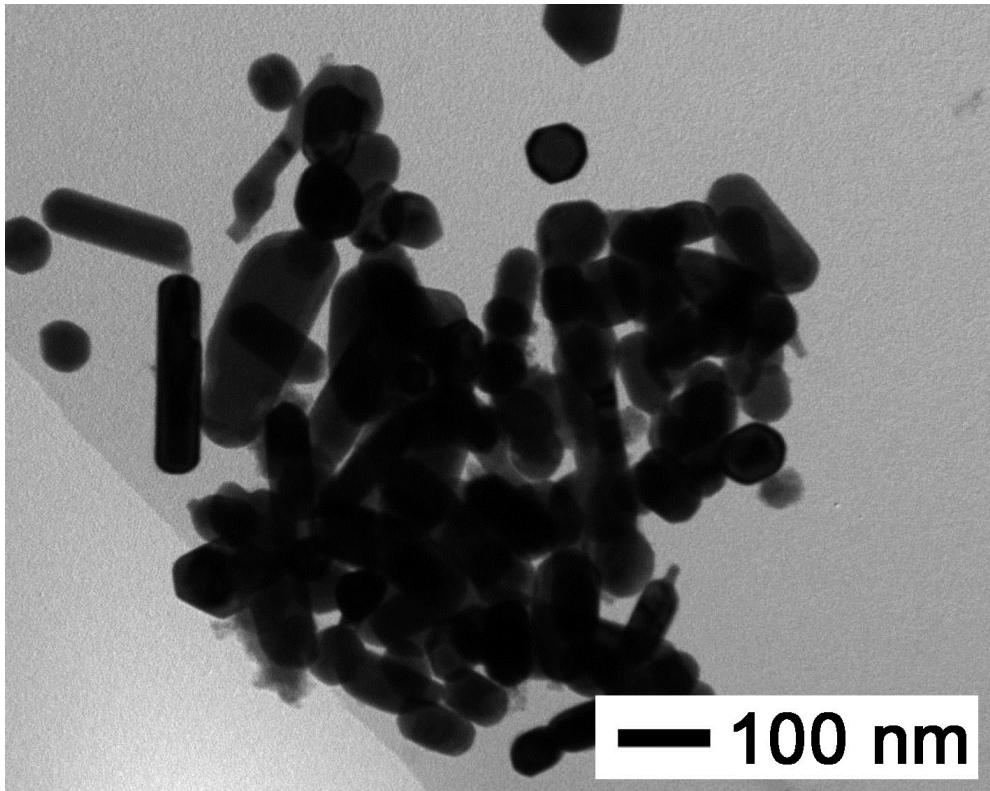


Figure S6. PbTe nanorod transformed from thin, long Te nanorod at 160 °C.

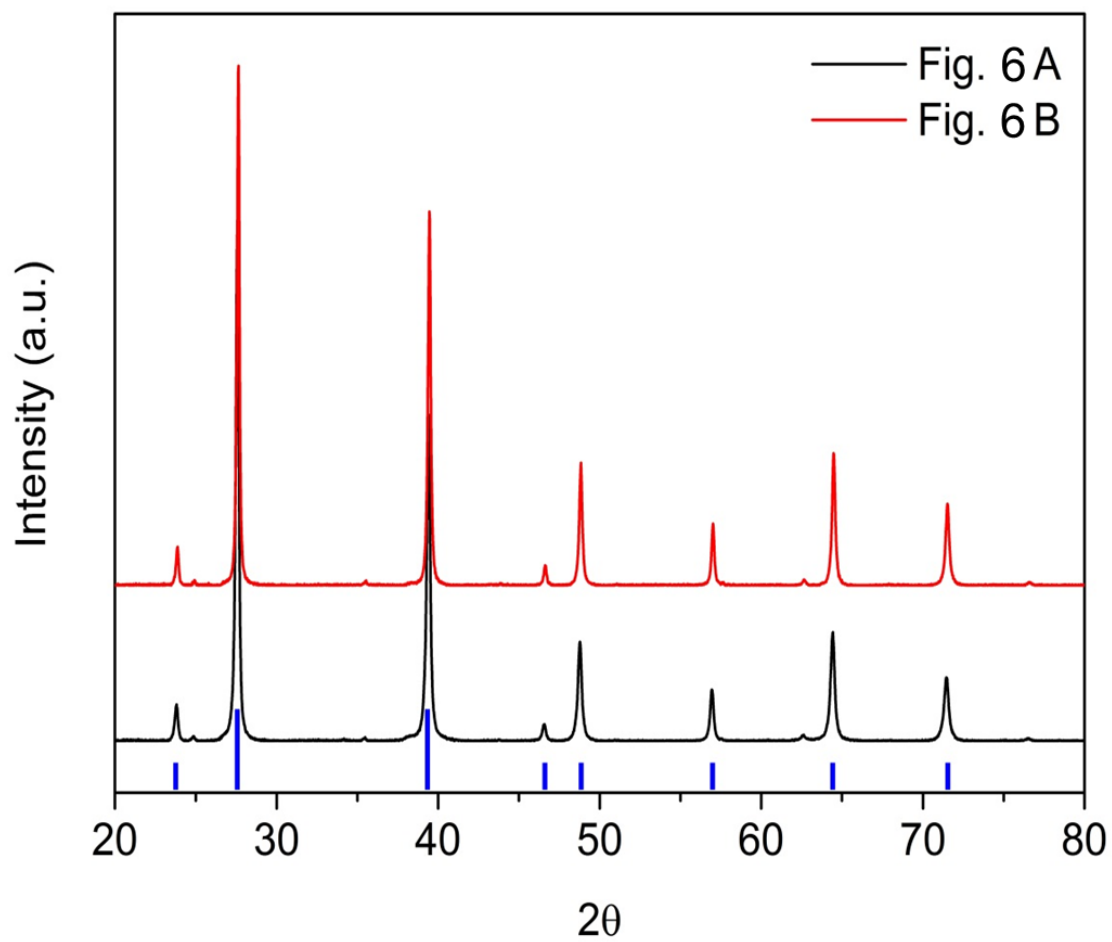


Figure S7. X-ray diffraction result of PbTe nanostructures in Figure 6.

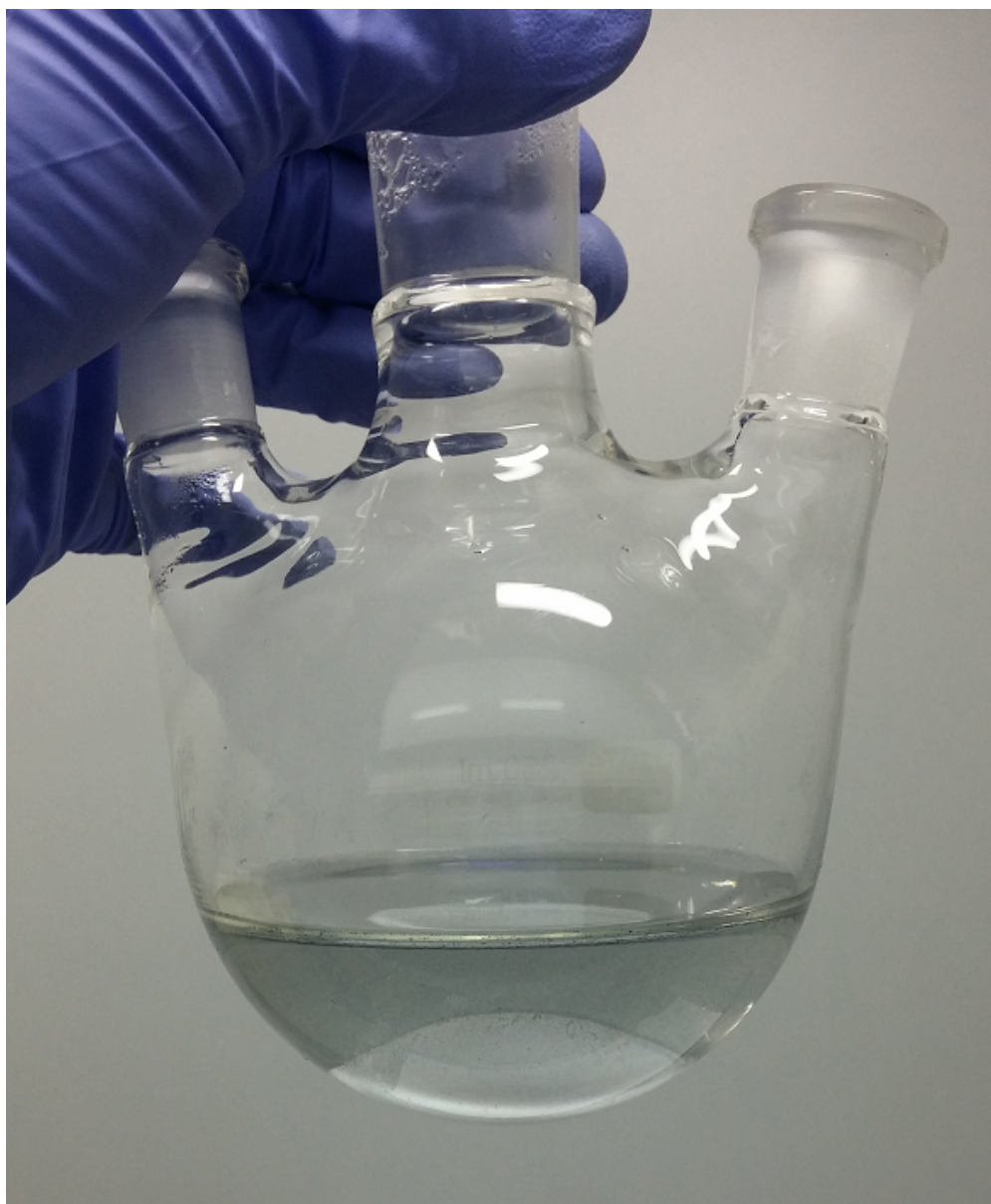


Figure S8. Supernatant solution after reducing the unreacted Te by excessive amount of hydrazine solution. The supernatant solution was collected by centrifuge from a batch for pure Te nanorods which was at 100 °C for 150 min.